ELSEVIER

Chemical Engineering Journal 70 (1998) 25–35

Chemical Engineering Journal

An experimental study on bulk and solution polymerization of methyl methacrylate with responses to step changes in temperature

Pallab Ghosh *, Santosh K. Gupta, D.N. Saraf

Department of Chemical Engineering, Indian Institute of Technology, Kanpur, 208 016, India

Received 25 April 1997; revised 28 November 1997; accepted 17 December 1997

Abstract

Several important polymerizations [e.g., polymethylmethacrylate (PMMA), polystyrene (PS), etc.] exhibit the gel, glass and cage effects during polymerization. These are associated with the decrease of the diffusivities of the macroradicals, monomer molecules and primary radicals with increasing viscosities of the reaction mass. The recent model of Seth and Gupta [V. Seth, S.K. Gupta, J. Polym. Eng., 15 (1995) 283.] has been used to explain these results. The model parameters are tuned using experimental data on near-isothermal bulk and solution polymerizations of methyl methacrylate (MMA) in a 1-l stainless steel, computer controlled reactor. A series of bulk and solution polymerizations (at 10%, 20% and 30% solvent concentrations) have been carried out at two different temperatures (50°C and 70°C) using benzoyl peroxide (BPO) as initiator at one initiator concentration (41.3 mol/m^3). Two important process variables, e.g., monomer conversion and viscosity average molecular weights were measured using gravimetric analysis and dilute solution viscometry, respectively. The results obtained from this study are in excellent agreement with those reported earlier in the literature. Experiments have also been carried out with step changes in temperature. Thus, the present study establishes the applicability of the model for the more general non-isothermal reactor operations with bulk as well as solution polymerizations along with semi-batch reactor operations.

Keywords: Polymerization; MMA; Modeling; Optimization

1. Introduction

Non-isothermal and semi-batch operations are quite common in industrial free-radical polymerization [e.g., polymethyl methacrylate (PMMA), polystyrene (PS), etc.] reactors. A fundamental understanding of the physico–chemical phenomena is required to incorporate these effects in a model, specially of the gel or Trommsdorff effects [1,2] where the reactions (Table 1) become diffusion-controlled and evaluation of the overall rate constants becomes difficult. Various attempts to model these effects have been reviewed by O'Driscoll [3], Hamielec [4], Mita and Horie [5] and Achilias and Kiparissides [6,7]. The phenomenological model of Chiu et al. [8] incorporates diffusional limitations as an integral part of the termination and propagation reactions. The appearance of this model led to several studies [9–11] on the optimization and parametric sensitivity of PMMA reactors. This model was extended by Achilias and Kiparissides [6,7] using the diffusion theory of Vrentas and Duda [12] and the theory of excess chain mobility [13]. The theory of Ray et al. [14] extends this work to apply it to semi-batch reactors and reactors operating under non-isothermal operations. These workers assumed that the initiator efficiency, f, remains constant as the monomer conversion increases. Seth and Gupta [15] improved on the model of Ray et al. by allowing the value of 'f' to decrease at high conversion. The

Table 1
Kinetic scheme for polymerization of MMA

Initiation	$I \xrightarrow{k_d} 2R$
Propagation	$R + M \xrightarrow{k_i} P_1$
Propagation	$P_n + M \xrightarrow{k_p} P_{n+1}$
Termination by combination	$P_n + P_m \xrightarrow{k_{tc}} D_{n+m}$
Termination by disproportionation	$P_n + P_m \xrightarrow{k_{td}} D_n + D_m$
Chain transfer to monomer	$P_n + M \xrightarrow{k_f} P_1 + D_n$
Chain transfer to monomer	$P_n + S \xrightarrow{k_s} S\cdot + D_n$
via solvent	$S\cdot + M \xrightarrow{fast} S + P_1$ or $P_n + M \xrightarrow{k_s} D_n + P_1$

* Corresponding author. Dept. of Chem. Eng., Indian Inst. of Tech., Bombay Powai, Mumbai 400076 India.

1385-8947/98/$19.00
PII S1385-8947(98)00064-3

new model is found to be less sensitive to minor variations in the values of the parameters. The robustness of this model is useful for developing optimal control strategies for such reactors.

However, several questions remain unanswered in these models. For example, Faldi et al. [16,17] have recently measured diffusion coefficients of large and small molecules in polymeric solutions using forced Rayleigh scattering and field gradient NMR under conditions simulating those encountered during the polymerization of MMA. They inferred that the diffusion coefficients of polymeric radicals, P_n, and primary radicals, R, decrease significantly during polymerization as the monomer concentration decreases significantly during polymerization as the monomer conversion increases. These decreases correlate well with the decrease of the termination constant, k_t, and the initiator efficiency, f, with increasing monomer conversions. This justifies the use of models (e.g., Refs. [6–8,14,15]) attempting to relate k_t and f with the diffusion coefficients. In contrast, the experimental values of the diffusion coefficients of a monomer do not decrease as rapidly as does the rate of propagation, k_p. They claimed that the success of models correlating k_p with the diffusion coefficients of the monomer is purely fortuitous. They, unfortunately, have not suggested models for k_p, and one, therefore, continues to use semi-empirical models for the glass and gel effects, even though they have been only partly substantiated by the fundamental studies of Faldi et al.

With an appropriate model available for free-radical polymerizations, one can now think of studying the *on-line* optimizing control of these processes. An important step in such studies is the measurement of the *state* of the system at different times, t. Densitometers and gel permeation chromatography (GPC) have been used in some experimental control studies [18–20] of solution polymerizations for estimating monomer conversions, $x(t)$, and the number average chain lengths, $\mu_n(t)$ [or the weight average chain lengths, $\mu_w(t)$]. However, these experimental techniques cannot be used conveniently for bulk polymerizations, and inferential state estimation techniques have been resorted to. Seth and Gupta [15], Chakravarthy et al. [21] and Bhargava Ram et al. [22] have suggested the use of experimental values of the viscosity, $\eta(t)$, of the reaction mass [along with the measured values of the temperature $T(t)$] for such purposes. Very recently, Mankar et al. [23] have experimentally estimated on-line viscosity of the reacting mass in bulk polymerization of methyl methacrylate at 50°C with azobisdiisobutyronitrile (AIBN) as initiator in a HAAKE® viscometer cum reactor. A very interesting feature of this on-going work is that a large number of experimental data points are available up to high monomer conversions ($\sim$65%). A definite correspondence between the $\eta(t)$ and $x(t)$ plots can be seen from these experiments.

There have been several experimental studies [18,19,24] on the control of free radical polymerization reactors but all of them have been restricted to solution polymerizations. Bulk and solution polymerization studies have been reported by Schulz and Harborth [25] using benzoyl peroxide (BPO) as initiator and bulk polymerization studies were reported by Balke and Hamielec [26] using AIBN as initiator. However, all of these studies were made in small glass ampoule reactors where typical industrial reactor conditions like heat and mass transfer effects, mixing and vaporization are absent. Moreover, no work has been reported on the optimal control of these reactors using analytical models. The model parameters in the model of Seth and Gupta [15] were tuned using bulk and solution polymerization data of Schulz and Harborth [25] and bulk polymerization data of Balke and Hamielec [26]. The model was further validated using bulk polymerization data taken in a 1-l stainless steel, PC interfaced Parr® reactor [27–29] with AIBN as initiator at different temperatures and initiator concentrations. In addition to these, step changes in temperature [27] and initiator concentration [28] were also carried out. The model was found to predict experimental results reasonably well without further tuning of its parameters. The 'tuned' models need to be tested out for solution polymerizations which has not been done so far.

Since temperature and initiator concentrations are the two important control variables in free-radical polymerization systems, the model should be tested for step changes in these.

These idealized operations are sufficient for checking the validity of the models for more general situations. In the present study, the recent model [15] has been tested against bulk as well as solution polymerizations with step changes in temperature.

1.1. The model

The model of Ray et al. [14] assumed the initiator efficiency, f, to be constant with time, while k_p and k_t were modeled to account for their decrease at high monomer conversions. It was found that the results were very sensitive to small variations in the parameters, θ_t and θ_p, used by these workers. This sensitivity was removed by Seth and Gupta [15], who incorporated an equation for f, using a modification of the model of Achilias and Kiparissides [7]. Table 2 gives the final equations [15] describing the gel, glass and cage effects, which need to be used along with appropriate mass-balance and moment equations [15]. This table also includes the best-fit correlations for θ_t and θ_p (applicable to both MMA–BPO–Bz bulk and solution polymerization, as well as to MMA–AIBN bulk polymerization), obtained by curve-fitting the isothermal data of Schulz and Harborth [25] and Balke and Hamielec [26] taken in small ampoules. Since these equations involve only *instantaneous* values of variables, they apply to any reactor, operating under non-isothermal conditions. The correlations for θ_t and θ_p are those obtained by Seth and Gupta [15]. The correlation for θ_f for the AIBN–MMA system, also, is the same as in Ref. [15]. The correlation for θ_f for the MMA–BPO–Bz system has been obtained in this study, using a curve-fit of the experimental data of Schulz and Harborth [25].

Table 2
Gel, glass and cage effect equations [15]

$$\frac{1}{f}=\frac{1}{f_0}\left[1+\theta_t(T)\frac{M}{V_1}\frac{1}{\exp[\xi_{13}\{-\psi+\psi_{ref}\}]}\right] \quad (a)$$

$$\frac{1}{k_t}=\frac{1}{k_{t,0}}+\theta_t(T)\mu_n^2\frac{\lambda_0}{V_1}\frac{1}{\exp[-\psi+\psi_{ref}]} \quad (b)$$

$$\frac{1}{k_p}=\frac{1}{k_{p,0}}+\theta_p(T)\frac{\lambda_0}{V_1}\frac{1}{\exp[\xi_{13}\{-\psi+\psi_{ref}\}]} \quad (c)$$

$$\psi=\frac{\gamma\left\{\frac{\rho_m\phi_m\hat{V}_m^*}{\xi_{13}}+\frac{\rho_s\phi_s\hat{V}_s^*}{\xi_{23}}+\rho_p\phi_p\hat{V}_p^*\right\}}{\rho_m\phi_m\hat{V}_m^*V_{fm}+\rho_s\phi_s\hat{V}_s^*V_{fs}+\rho_p\phi_p\hat{V}_p^*V_{fp}} \quad (d)$$

$$\psi_{ref}=\frac{\gamma}{V_{fp}} \quad (e)$$

$$\xi_{13}=\frac{\hat{V}_m^*(MW_m)}{\hat{V}_p^*M_{jp}} \quad (f)$$

$$\xi_{23}=\frac{\hat{V}_s^*(MW_s)}{\hat{V}_p^*M_{jp}} \quad (g)$$

$$\xi_{13}=\frac{\hat{V}_I^*(MW_I)}{\hat{V}_p^*M_{jp}} \quad (h)$$

$$k_d=k_d^0\exp(-E_d/RT) \quad (i)$$

$$k_{p,0}=k_{p,0}^0\exp(-E_p/RT) \quad (j)$$

$$k_{t,0}=k_{td,0}^0=k_{td,0}\exp(-E_{td}/RT) \quad (k)$$

Best-fit correlation (BFCs) for the MMA–AIBN or MMA–BPO system [15]

$$\log_{10}[\theta_t(T),s]=1.241\times10^2-1.0314\times10^5(1/T)+2.2735\times10^7(1/T^2) \quad (l)$$

$$\log_{10}[\theta_p(T),s]=8.03\times10^1-7.50\times10^4(1/T)+1.765\times10^7(1/T^2) \quad (m)$$

For AIBN–MMA system (bulk polymerization) [15]

$$\log_{10}[10^3\theta_t(T),m^3\ mol^{-1}]=2.016\times10^2-1.455\times10^5(1/T)+2.70\times10^7(1/T^2) \quad (n)$$

For BPO–MMA system (bulk and solution polymerization) [this work]

$$\log_{10}[10^3\theta_t(T),m^3\ mol^{-1}]=-40.86951+1.7179\times10^4(1/T) \quad (o)$$

Other details provided in Refs. [14,15].

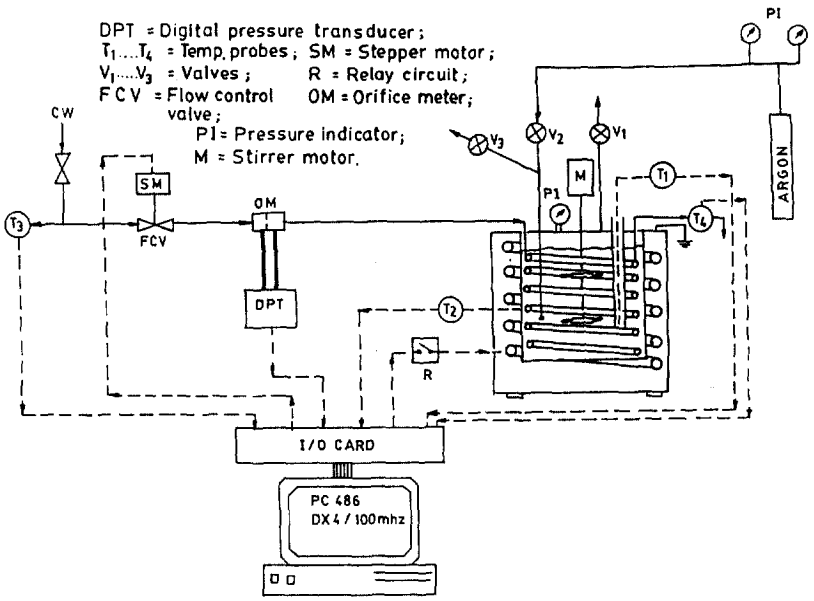

Fig. 1. Schematic diagram of experimental set-up.

2. Experimental

The polymerization was carried out in a 1-l stainless steel PC interfaced Parr reactor (Parr Instrument, Moline, IL, USA). The experimental set-up which includes the computer and its peripherals, sensors, transducers and actuators in addition to the Parr reactor assembly is shown in Fig. 1. Later in this section, we describe the monomer and initiator treatment procedures and polymerization techniques as well as their final analysis, in brief.

2.1. Purification of monomer

LR grade methyl methacrylate (MMA) (Central Drug House (P), Mumbai, India) was purified prior to use. The monomer was washed three times with equal volumes of a 5% NaOH (GPR, BDH, Mumbai, India) solution in water to remove the phenolic stabilizers [quinol (hydroquinone), 0.01%] present in it. The mixture was allowed to settle in a separating funnel forming two layers, the bottom inorganic layer was discarded leaving the monomer. The MMA was then washed at least three times with equal volumes of doubly distilled water to remove traces of NaOH. Settling times of at least 2 h after each NaOH and water wash were allowed. The residual water was removed from the monomer by passing it through beds (placed in series) of molecular sieves (type 30-541, 4–5 Å, Linde Division, Union Carbide, USA) and silica gel blue (LR, coarse, mesh 3–8, NICE, Kochi, Kerala, India). Fresh batches of regenerated silica gel and molecular sieves (by washing and drying in an oven at 70°C for 5 h) were used for every 250 ml of monomer. The regenerated drying agents (silica gel regains its original blue color after drying) were stored in air tight containers.

The monomer obtained after the above steps was distilled under vacuum ($P = 50$ mm Hg) at about 30°C (room temperature). Ice cold water was circulated in the condenser which helped in condensing the distillate monomer. A few beads of molecular sieves were added into the distillation flask to augment flashing of the monomer under vacuum. The distilled monomer was stored in a refrigerator over fused $CaCl_2$ (Loba Chemie, Mumbai, India) in a desiccator. The final yield of the pure monomer was about 50% of the original sample.

2.2. Initiator

The initiator, benzoyl peroxide (BPO) (LR, Central Drug House (P)) was recrystallized from acetone (AR, Ranbaxy Labs., S.A.S. Nagar, Punjab, India). A saturated solution of BPO was prepared (at room temperature) in a conical flask by mixing an excess of BPO. The solution was filtered (using ordinary filter paper). The filtrate was chilled in a refrigerator to crystallize the BPO. The shiny crystals of BPO were recovered by filtration. The crystals were dried in a vacuum oven at room temperature (heating causes thermal decomposition, BPO decomposes at ~ 108°C). The mother liquor was stored to be used for crystallization in future.

2.3. Batch polymerization

(1) BPO was dissolved in a measured amount of MMA [with benzene (AR, Ranbaxy Labs.) in case of solution polymerizations] to achieve the desired initiator concentration in a 1-l volumetric flask. The solution was thoroughly mixed to ensure complete dissolution of initiator (which is quite soluble in the monomer as well as in benzene).

(2) The solution was transferred to the Parr reactor. The reactor was carefully closed with the head and sealed with the half-rings and the steel retaining ring. All the valves were closed. The reactor contents were degassed by applying vac-

uum ($P=5$ mm Hg) through the gas release valve for about 30 min. The vacuum pump (model 150 D, Leo Engineering, Kalletumkara, Kerala, India) was connected to the reactor through ice-traps to remove any condensable in the gas. After degassing, the reaction mass was pressurized with argon (IOL-AR-2, Indian Oxygen, New Delhi, India) charged through the gas-charge valve. After about 20 s of the commencement of this operation the valve connected to the pressure gauge line was opened. Once the desired pressure of about 900 kPa was achieved, the gas charge valve was closed. Argon was re-charged during a run if the pressure fell below 850 kPa.

(3) All the peripheral connections (temperature sensors, etc.) to the reactor–PC setup (Fig. 1) were checked and activated. The controller parameters and desired set point were supplied as inputs to the control program. Samples were withdrawn at regular intervals of time through the sample collection port [valve V_3 in Fig. 1]. The sampling times were decided by the expected dynamics of the system. Samples of about 3 ml were collected in 50-ml sample bottles containing weighed amounts of solvent [~ 10 ml of benzene and trace amounts of inhibitor (hydroquinone)]. The sample bottles were kept ice-cold in order to freeze the reaction as soon as the sample was collected. Before drawing the sample, about 2 ml of the sample coming out of the port was discarded, this being the estimated hold-up of material in the sample line. This procedure ensured that the samples drawn were really representative of the reaction mixture. The copper tube connected to the sample collecting port was cleaned with dichloromethane (AR, Ranbaxy Labs.) and dried before reuse. Sample bottles were reweighed to calculate the mass of the sample drawn. The occurrence of the gel effect can be inferred from the sudden change in the consistency of the material flowing out. During this period, samples were collected as soon as possible. It was found that the argon pressure of about 10 atm above the liquid reaction mass was unable to push out the liquid through the sample port shortly after the onset of the gel effect due to very high viscosity ($\sim 11{,}000$ Pa s) [23].

(4) The reaction was stopped as soon as the stirrer stopped due to the high viscosity of the reaction mixture. After the reaction was complete, the reactor pressure was released slowly by opening the gas release valve and the reactor was then opened. A few samples were taken out from the opened reactor near the stirrer at different intervals and quenched as described before. Since the time span for the collection of these samples is only a few minutes, the temperature of the reaction mass around the stirrer does not go down significantly during this period and reasonably accurate estimates of monomer conversion and the viscosity average molecular weight can be obtained. These samples were representatives of the higher conversion ranges. Then the reactor was allowed to cool down to room temperature and then dichloromethane was added to it for dissolution of the polymer. A considerable amount of polymer was removed mechanically also.

2.4. Analysis of monomer conversion and molecular weight

The monomer conversion was estimated gravimetrically [26]. The polymer was precipitated from the solution in the sample tube by adding about 100 ml of methanol (non-solvent). The precipitated polymer was filtered through a dried and pre-weighed filter paper (Whatman 41, Whatman, Maidstone, UK). The polymer was dried at 50°C under vacuum ($P=5$ mm Hg) for about 24 h (tested to be sufficiently long to ensure complete drying). The mass of the precipitated polymer was found by weighing the filter paper again. The polymer samples were stored in a desiccator till molecular weight analysis was done.

The viscosity average molecular weights, M_v, of polymer samples were determined by dilute solution viscometry [30–32]. Efflux times through the capillary of the viscometer (Ubbelhode viscometer No. 501 01, Schott-Gerate, Hofheim, West Germany) were estimated. From these measurements, the intrinsic viscosities for each sample were calculated.

The M_v is calculated from the Mark–Houwink equation,

$$[\eta] = K M_v^a \tag{1}$$

The values of the constants, 'K' and 'a', were taken from the Polymer Handbook [33] for the PMMA–Bz system at 30°C. The following values of 'K' and 'a' were used for the calculations:

$$K = 5.2 \times 10^{-5} \text{ dl/g}$$
$$a = 0.76 \tag{2}$$

These constants are quite insensitive to small changes in temperature.

3. Results and discussion

A series of experiments on bulk and solution polymerization of methyl methacrylate with different temperature histories [near isothermal, step decrease (SD) and step increase (SI)] at a fixed initiator loading of 41.3 mol/m^3, have been conducted. Two important process output variables, namely, monomer conversion, x, and average molecular weight, M_v, as determined from intrinsic viscosity, have been measured at different sampling times during the course of polymerization. Table 3 lists the controller parameters along with the curve-fitted expressions for the experimental temperature histories in all the runs conducted.

Near isothermal (NI) runs were conducted at 50°C and 70°C for solvent concentrations of 0% (bulk), 10%, 20% and 30% [(Runs N150FS0, NI50FS10, NI50FS20, NI50FS30, NI70FS0, NI70FS10, NI70FS20 and NI70FS30); FS indicates volume fraction (%) of solvent]. The conditions are referred to as *near isothermal* due to the fact that the reactor system takes about 6 to 10 min to attain the desired polymerization temperature. For NI70FSx runs ($x \equiv 0$, 10, 20, 30), the reaction mass was first preheated approximately to 45°C and thereafter the control started. This was done due to the

Table 3
Details of experimental runs

No.	Run no.	K_c^h [a]	τ_t^h	K_c^c	τ_t^c	Exp. temp. history [T (°C), t (min)]
1	NI50FS0	0.07	900	−70	90	$T=23.81+2.038t+0.295t^2-2.303\times10^{-2}t^3$; $t\le9.71$ $=50$; $t>9.71$
2	NI50FS10	0.07	900	−70	90	$T=32.95+6.424t-1.063t^2+0.103t^3$; $t\le5.03$ $=50$; $t>5.03$
3	NI50FS20	0.07	900	−70	90	$T=27.73+1.150t+0.611t^2-4.04\times10^{-2}t^3$; $t\le6.70$ $=50$; $t>6.7$
4	NI50FS30	0.07	900	−70	90	$T=34.93+3.652t+0.366t^2-7.539\times10^{-2}t^3$; $t\le4.02$ $=50$; $t>4.02$
5	NI70FS0	0.08	900	−65	90	$T=44.45+5.576t-0.332t^2+2.78\times10^{-3}t^3$; $t\le10.04$ $=70$; $t>10.04$
6	NI70FS10	0.08	900	−65	90	$T=44.94+5.52t-0.459t^2+1.636\times10^{-2}t^3$; $t\le10.16$ $=70$; $t>10.16$
7	NI70FS20 a	0.08	900	−65	90	$T=47.23+5.572t+0.135t^2-6.152\times10^{-2}t^3$; $t\le5.03$ $=70$; $t>5.03$
8	NI70FS20 b	0.08	900	−65	90	$T=44.76+4.61t+0.025t^2-2.421\times10^{-2}t^3$; $t\le7.03$ $=70$; $t>7.03$
9	NI70FS30 a	0.08	900	−65	90	$T=44.85+4.89t-0.026t^2-2.413\times10^{-2}t^3$; $t\le7.37$ $=70$; $t>7.37$
10	NI70FS30 b	0.08	900	−65	90	$T=44.74+4.90t-0.039t^2-3.672\times10^{-2}t^3$; $t\le7.37$ $=70$; $t>7.37$
11	SIFS10	0.07	900	−70	90	$T=27.49+0.524t-0.635t^2-4.67\times10^{-2}t^3$; $t\le9.05$ $=50$; $9.05<t\le128.03$ $=-232.02-1.065t+4.95\times10^{-2}t^{-2}-1.87\times10^{-4}t^3$; $128.03<t\le137.41$ $=70$; $t>137.41$
12	SDFS10	0.07	900	−70	90	$T=41.59+3.757t+0.404t^2-0.054t^3$; $t\le7.37$ $=70$; $7.3665<t\le57.25$ $=69.31+1.144t-1.028\times10^{-3}t^2-3.207\times10^{-4}t^3$ $57.25<t\le64.89$ $=50°C$; $t>64.89$

[a] The units of K_c^h, K_c^c and τ_t are (°C/full power)$^{-1}$, [°C/(g/min)]$^{-1}$ and min respectively.

fact that, in winter, when the room temperature is quite low ($\sim$ 10°C), it takes a long time to reach 70°C from such a low room temperature and the actual reaction hardly starts before 40°C. Vaporization of the monomer is prevented by applying pressure of about 1400 kPa absolute, using argon. The argon pressure also helps in driving out samples of the reaction mass through the sample collection port.

In all these runs, there is an initial heating period when the temperature changes from the ambient to the desired value of 50 or 70°C, followed by a near constant temperature. The transient was fitted with a polynomial in a least-squares sense. The fitted equation for each run is given in Table 3. Fig. 2 shows the temperature history for the NI50FS0 run. The conversion (x) vs. time (t) plots for the NI50FS0, NI50FS10 and NI50FS20 runs are shown in Figs. 3–5 while Figs. 6–8 show similar results for the near isothermal (NI) runs at 70°C at 0, 20 and 30% solvent concentrations [NI70FS0, NI70FS20 and NI70FS30 runs]. Some of the molecular weight measurement results as a function of conversion (x) are given in Figs. 9 and 10 for the NI50FS0 and NI70FS0 runs. The NI70FS20 and NI70FS30 runs were repeated to establish the reproducibility of the results. The conversion vs. time runs for 0 and 20% solvent concentrations match quite well with those reported by Schulz and Harborth [25].

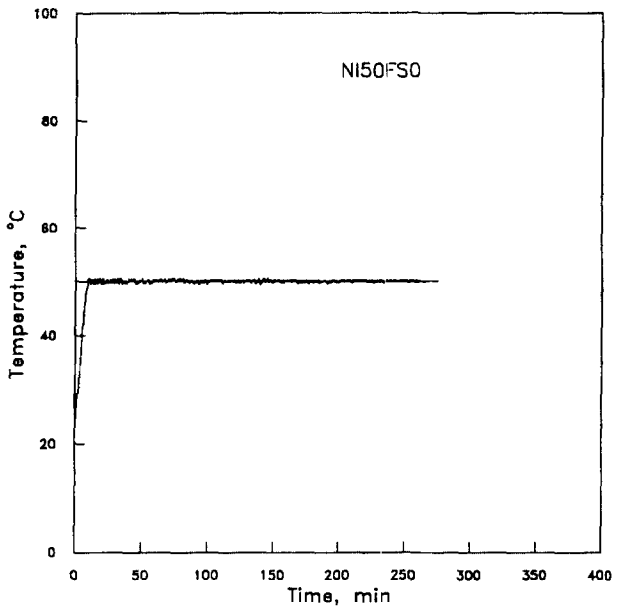

Fig. 2. Temperature history for the NI50FS0 run.

The results of Schulz and Harborth are shown in these plots for comparison.

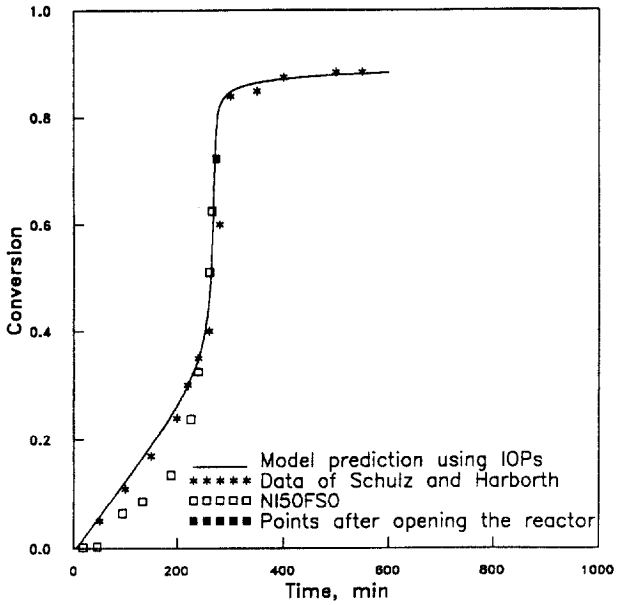

Fig. 3. Conversion history for the NI50FS0 run. Solid line indicates the model prediction using the new IOPs. Data of Schulz and Harborth [25] are also shown for comparison.

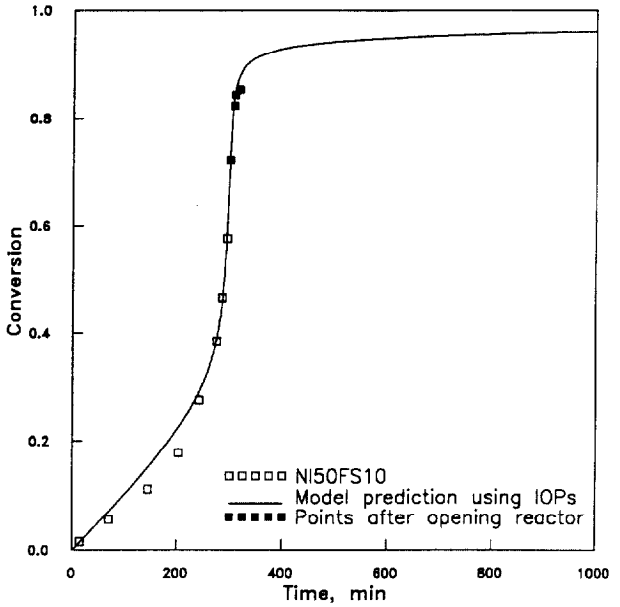

Fig. 4. Conversion history for the NI50FS10 run. Solid line indicates the model prediction using the new IOPs.

It was found necessary to retune the model-parameters obtained by Seth and Gupta [15] using the NI50FSx and NI70FSx runs. The individually optimized parameters (IOPs, θ_t, θ_p, θ_f), were obtained using our reactor data *only* with the *actual* temperature histories. The objective function used was

$$\text{Min } E(\theta_t,\theta_p,\theta_f) = \sum_{i=1}^{N}\left[\frac{x_i^{\exp} - x_i^{\text{th}}}{x_i^{\exp}}\right]^2$$

The NAG library (Mark 14) program E04UPF [which implements sequential quadratic programming (SQP) and specially designed to minimize objective functions of the type involving sum of square errors] was used to obtain the IOPs.

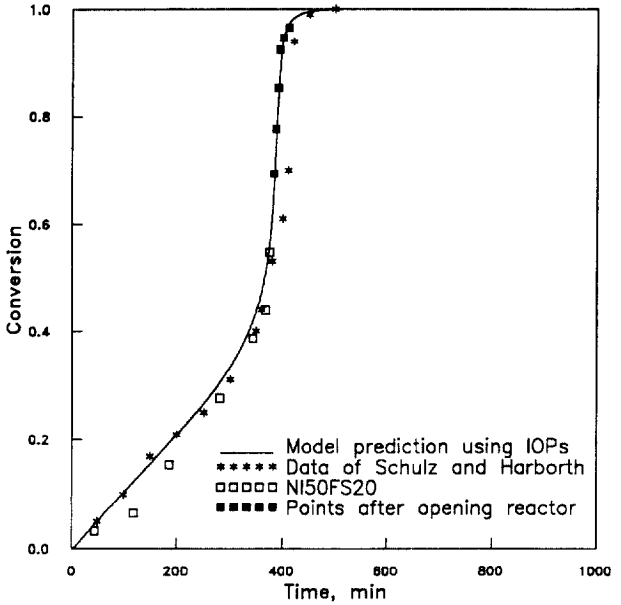

Fig. 5. Conversion history for the NI50FS20 run. Solid line indicates the model prediction using the new IOPs. Data of Schulz and Harborth [25] are also shown for comparison.

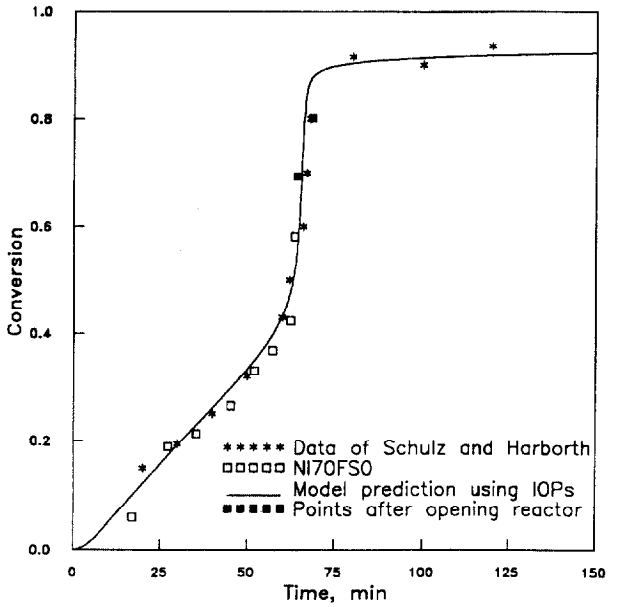

Fig. 6. Conversion history for the NI70FS0 run. Solid line indicates the model prediction using the new IOPs. Data of Schulz and Harborth [25] are also shown for comparison.

The three curve-fit parameters, θ_t, θ_p and θ_f, of the model [15] were obtained for all the eight cases and these IOPs are listed in Table 4. Table 4 also includes the IOPs obtained by Seth and Gupta [15] for AIBN bulk polymerization data of Balke and Hamielec [26]. The best-fit correlations (BFCs) for θ_t, θ_p and θ_f given in Table 2 are used to generate values for the individual runs, both for the MMA–AIBN and MMA–BPO–Bz system. These are also given in Table 4. It may be emphasized that for the MMA–BPO–Bz system, the IOP values in Table 4 have been generated using our own experimental data taken in a 1-l reactor. In contrast to these, the

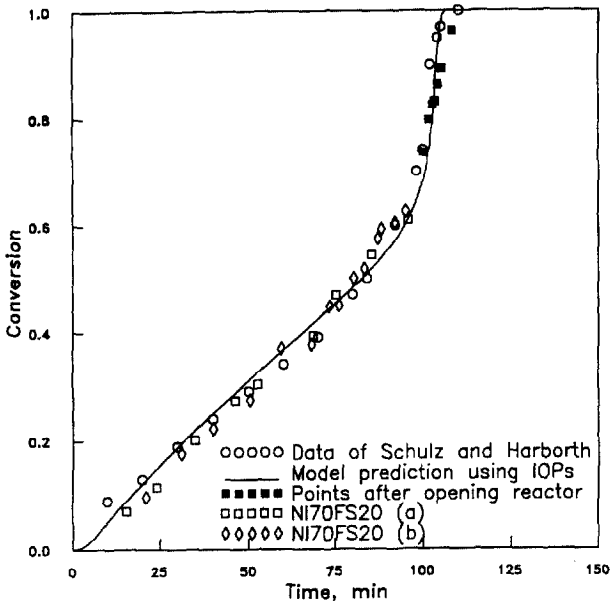

Fig. 7. Conversion histories for the NI70FS20 (a and b) runs. Solid line indicates the model prediction using the new IOPs. Data of Schulz and Harborth [25] are also shown for comparison.

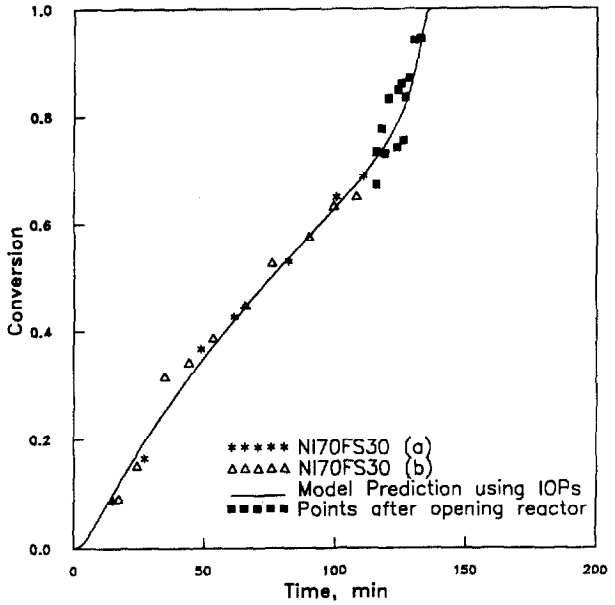

Fig. 8. Conversion histories for the NI70FS30 (a and b) runs. Solid line indicates the model prediction using the new IOPs.

BFCs for this system (given in Table 2) have been obtained using isothermal data of Schulz and Harborth [25] in *small ampoules*. A super-global curve-fit using all the experimental data ([25,26] and this work) could be performed in the future. The CPU time taken ranged between 20–25 s for all these runs on a super-mini HP 9000/735 mainframe computer.

The next phase of the work was to obtain experimental data using step changes in temperature [step increase (SI) and step decrease (SD)] at different times and compare them with predictions from the model. Polymerization of MMA with 10% benzene [with the same initiator concentration as

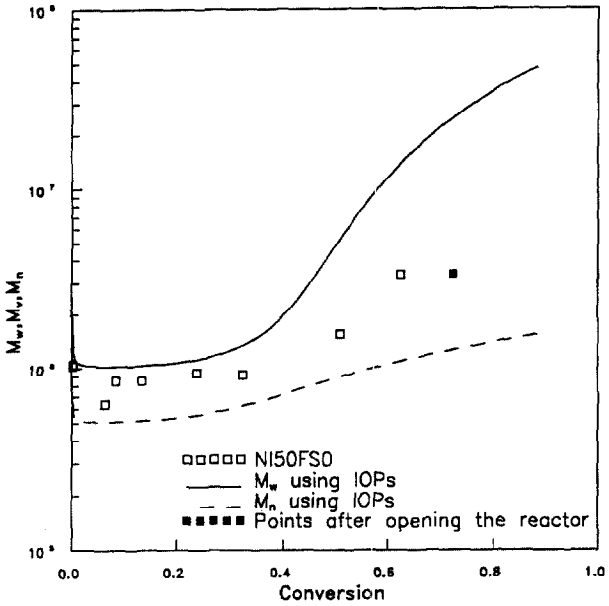

Fig. 9. Molecular weight vs. conversion (x) for the NI50FS0 run.

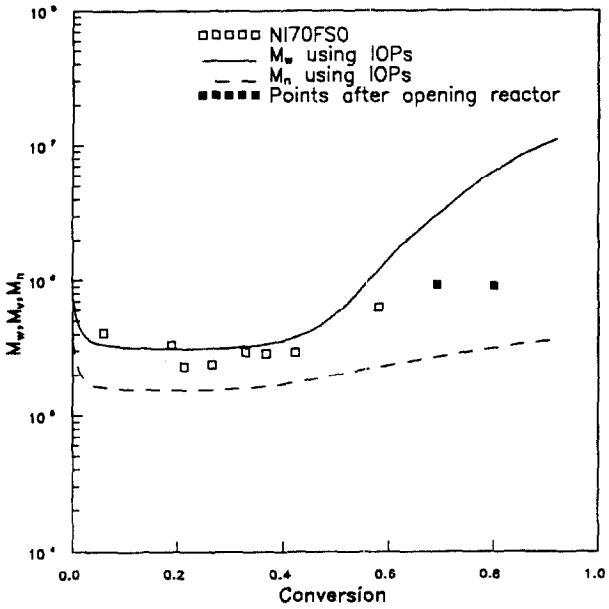

Fig. 10. Molecular weight vs. conversion (x) for the NI70FS0 run.

earlier] was carried out at 50°C for 128 min (like the NI50FS10 run) and then suddenly the temperature was increased from 50°C to 70°C and was kept there till the reaction was over. The conversion results from the SIFS10 run are shown in Fig. 11. The model prediction (without returning the IOPs in Table 4) is also shown by solid lines. The IOPs for the corresponding regions (50°C and 70°C) were used while generating the model predictions (it is assumed that the errors due to intermediate changes of T, are small). It can be seen that the model can predict the step increase quite accurately.

Step decrease was also done in a similar manner (run SDFS10). The temperature of the reactor was raised from room temperature to 70°C (like the NI70FS10 run), kept there for around 57 min and then suddenly decreased to 50°C

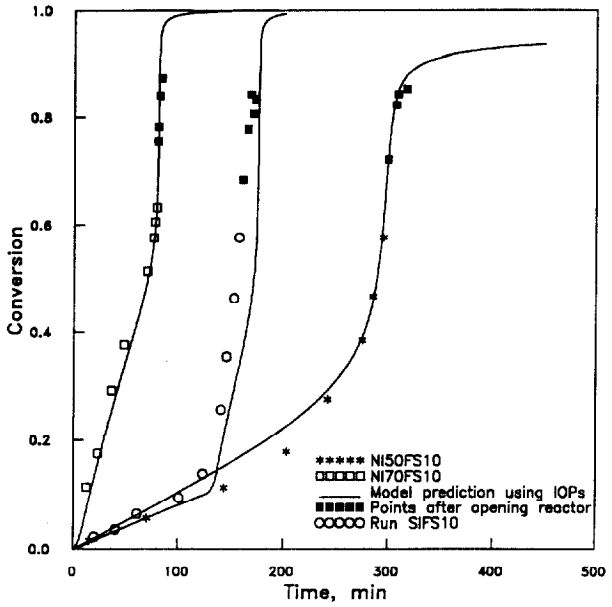

Fig. 11. Conversion history for the SIFS10 run. Solid lines indicate the model prediction using the new IOPs.

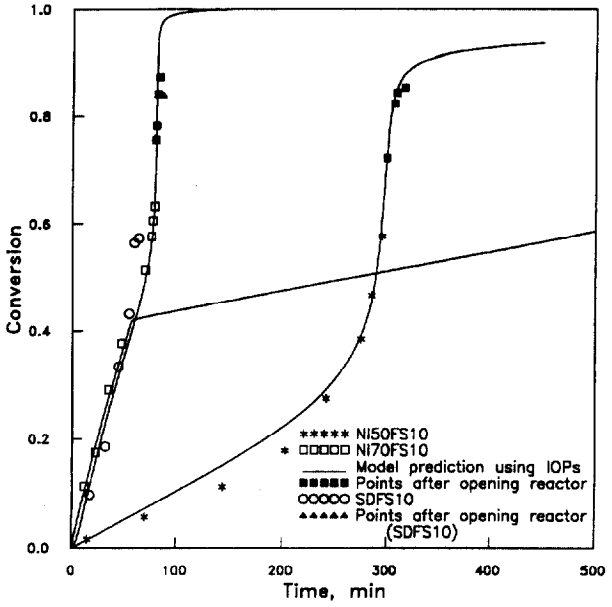

Fig. 12. Conversion history for the SDFS10 run. Solid lines indicate the model prediction using the new IOPs.

and kept there till the end. The conversion plot is shown in Fig. 12 along with the theoretical plot using the IOPs. It can be seen that the model predicts a postponement of the gel point in this case whereas the experimental results are almost identical to the results for the NI70FS10 run. A sharp decrease in temperature from 70°C to 50°C slows down the reaction rate resulting in a postponement of the gel effect. On the other hand, reduction in temperature leads to high molecular weight radicals which increases the viscosity of the reaction mass [$\eta \propto M_w^{3.4}$]. As a result of increase in viscosity in the reaction medium, the termination reaction becomes slower since mutual termination is the reaction between two large polymer radicals. However, the propagation reaction (involving a large polymer radical and a small monomer molecule) continues. Since molecular and segmental diffusion must occur before any chemical reaction, increase in viscosity of the reaction mass with conversion would reduce the segmental diffusion till mutual termination becomes diffusion controlled. Thus, the position of gel point in case of a step change in temperatures depends on these phenomena and the point of conversion at which the step change is effected. However, further experimental studies at several other points of conversion will explain the point further.

Table 4
IOPs and values from the BFCs for the individual runs for MMA polymerization

T(°C)	$[I]_0$ (mol/m^3)	f_s^0	N_t	N_c	IOP				BFC (Table 2)			
					θ_t (s)	θ_p (s)	$10^3\,\theta_f$ (m^3/mol)	E	θ_t (s)	θ_p (s)	$10^3\,\theta_f$ (m^3/mol)	G_E
50*	25.80	0.0	36	0	4.79×10^{22}	3.34×10^{17}	7.60×10^{9}	0.210				
	20.18	0.0	16	0	4.49×10^{22}	1.25×10^{17}	6.70×10^{9}	0.211	4.40×10^{22}	1.69×10^{17}	7.96×10^{9}	
	15.48	0.0	17	0	4.25×10^{22}	6.86×10^{17}	5.10×10^{9}	0.197				
70*	25.80	0.0	19	19	5.44×10^{16}	2.05×10^{11}	5.99×10^{6}	0.278	4.05×10^{16}	4.24×10^{11}	7.63×10^{6}	1.921
	15.48	0.0	12	12	4.64×10^{16}	8.27×10^{11}	2.86×10^{6}	0.223				
90*	25.80	0.0	18	18	3.79×10^{12}	4.89×10^{7}	2.46×10^{5}	0.232	3.02×10^{12}	4.07×10^{7}	4.72×10^{5}	
	15.48	0.0	11	11	3.13×10^{12}	5.40×10^{7}	7.23×10^{5}	0.158				
50**		0.0	13	0	5.24×10^{22}	5.01×10^{16}	3.05×10^{12}	0.052				
		0.1	12	0	6.42×10^{22}	2.08×10^{17}	9.20×10^{12}	0.086				
	41.30	0.2	13	0	6.68×10^{22}	1.03×10^{17}	8.20×10^{12}	0.033	4.40×10^{22}	1.69×10^{17}	1.96×10^{12}	
		0.3	14	0	6.82×10^{22}	1.15×10^{17}	8.22×10^{12}	0.037				
70**		0.0	10	0	5.79×10^{16}	6.11×10^{11}	4.01×10^{9}	0.022				
		0.1	12	0	4.55×10^{16}	8.25×10^{11}	9.76×10^{8}	0.126				2.786
	41.30	0.2	31	0	7.92×10^{16}	6.30×10^{11}	5.61×10^{9}	0.094	4.05×10^{16}	4.24×10^{11}	1.56×10^{9}	
		0.3	30	0	8.35×10^{16}	4.24×10^{11}	9.06×10^{8}	0.022				

* AIBN–MMA [15].
** BPO–Bz–MMA [this work].

4. Conclusions

A series of experiments on bulk as well as solution polymerization of MMA (with benzene as solvent and BPO as initiator), at a fixed initiator loading of 41.3 mol/m^3 have been conducted. The experimental results (conversion and average molecular weights) obtained show an excellent accord with the prediction from the theoretical model of Seth and Gupta [15]. The three model parameters, θ_t, θ_p, θ_f, were re-tuned using experimental data thus obtained. Also, the model has been found to predict the results with a step increase in temperature very well (without further tuning the parameters) while it failed to predict the results for the step decrease run accurately. The results validate the model for solution polymerizations as well as for bulk polymerizations. Further work on step changes in solvent concentration and/or initiator concentration along with temperature change will validate the theory to a larger extent.

5. Nomenclature

a	parameter in Mark–Houwink equation
D_n	dead polymer molecule
E	objective function
E_d, E_p, E_t	activation energies for initiation, propagation and termination in absence of gel or glass effects (kJ/mol)
f	initiator efficiency at time t
f_0	initiator efficiency in the limiting case of zero diffusional resistance
f_s^0	solvent concentration
I	initiator
$[I]_0$	initial concentration of initiator (initiator loading) (mol/m^3)
K	parameter in Mark–Houwink equation, dl/g
K_c^c	controller gain for cooling cycle, [°C/(g/min)]$^{-1}$
K_c^h	controller gain for heating cycle, (°C/full power)$^{-1}$
k_d, k_p, k_t	rate constants for initiation, propagation and termination in presence of the gel and glass effects (s^{-1} or m^3/mol/s)
k_d^0, $k_{p,0}^0$, $k_{t,0}^0$	frequency factors for initiation, propagation and termination in absence of gel and glass effects (s^{-1} or m^3/mol/s)
$k_{t,0}$, $k_{p,0}$	k_t and k_p in absence of gel and glass effects (m^3/mol/s).
M	moles of monomer in the liquid phase
M_{jp}	molecular weight of polymer jumping unit (kg/mol)
M_n	number average molecular weight (g/gmol) [$\equiv (MW_m)(\lambda_1+\mu_1)/(\lambda_0+\mu_0)$, kg/mol]
M_v	viscosity average molecular weight (g/gmol)
M_w	weight average molecular weight (g/gmol) [$\equiv (MW_m)(\lambda_2+\mu_2)/(\lambda_1+\mu_1)$, kg/mol]
(MW_I), (MW_m), (MW_s)	molecular weights of pure initiator, monomer and solvent (kg/mol)
N	number of experimental data points used in optimization
NI	near isothermal
NI50FSx	near isothermal (50°C) runs with solvent (benzene) concentration of x % [$x \equiv 0$, 10, 20 and 30]
NI70FSx	near isothermal (70°C) runs with solvent (benzene) concentration of x % [$x = 0$, 10, 20 and 30]
P_n	growing polymer radical having 'n' repeat units
R	primary radical
R	universal gas constant (kJ/mol/K)
S	moles of solvent (benzene used in this study)
S·	solvent radical
t	time (s or min)
T	temperature of reaction mixture at time t (K)
V_l	volume of liquid at time t (m^3)
V_{fm}, V_{fp}, V_{fs}	fractional free volumes of monomer polymer, and solvent in the reaction mixture.
$\hat{V}_l^*$, $\hat{V}_m^*$, $\hat{V}_p^*$, $\hat{V}_s^*$	specific critical hole free volume of initiator, monomer, polymer, and solvent (m^3/kg)
x	monomer conversion

Greek letters

γ	overlap factor
η	viscosity of reaction mass
θ_f, θ_p, θ_t	adjustable parameters in the model (m^3/mol, s, and s respectively)
λ_k	kth ($k = 0, 1, 2, \ldots$) moment of live (P_n) polymer radicals $\equiv \sum_{n=1}^{\infty} n^k P_n$ (mol)
μ_k	kth ($k = 0, 1, 2, \ldots$) moment of dead (D_n) polymer chains $\equiv \sum_{n=1}^{\infty} n^k D_n$ (mol)
μ_n	number average chain length at time $t \equiv (\lambda_1+\mu_1)/(\lambda_0+\mu_0)$
ξ_{13}, ξ_{23}, ξ_{13}	ratio of the molar volume of the monomer, solvent, and initiator jumping units to the critical molar volume of the polymer, respectively
ρ_m, ρ_p, ρ_s	density of pure (liquid) monomer, polymer or solvent at temperature T (at time t) (kg/m^3)

τ_I^c	integral time constant of the process in cooling cycle, min
τ_I^h	integral time constant of the process in heating cycle, min
ϕ_m, ϕ_p, ϕ_s	volume fractions of monomer, polymer, or solvent in liquid at time t
ψ, ψ_{ref}	defined in Eqs. (d) and (e) in Table 2

References

[1] E. Trommsdorff, H. Köhle, P. Lagally, Makromol. Chem. 1 (1947) 169.
[2] R.G.W. Norrish, R.R. Smith, Nature 150 (1942) 336.
[3] K.F. O'Driscoll, Pure Appl. Chem. 53 (1981) 617.
[4] A.H. Hamielec, Chem. Eng. Commun. 24 (1983) 1.
[5] I. Mita, K.J. Horie, Macromol. Sci., Rev. Macrom. Chem. Phys. C27 (1987) 91.
[6] D.S. Achilias, C.J. Kiparissides, J. Appl. Polym. Sci. 35 (1988) 1303.
[7] D.S. Achilias, C.J. Kiparissides, Macromolecules 25 (1992) 3739.
[8] W.Y. Chiu, G.M. Carratt, D.S. Soong, Macromolecules 16 (1983) 348.
[9] B. Kapoor, S.K. Gupta, A. Varma, Polym. Eng. Sci. 29 (1989) 1246.
[10] N.R. Vaid, S.K. Gupta, Polym. Eng. Sci. 31 (1991) 1708.
[11] B.M. Louie, D.S. Soong, J. Appl. Polym. Sci. 30 (1985) 3707.
[12] J.S. Vrentas, J.L. Duda, AIChE J. 25 (1979) 1.
[13] S.K. Soh, D.C. Sundberg, J. Polym. Sci., Polym. Chem. Edn. 20 (1982) 1315.
[14] A.B. Ray, D.N. Saraf, S.K. Gupta, Polym. Eng. Sci. 35 (1995) 1290.
[15] V. Seth, S.K. Gupta, J. Polym. Eng. 15 (1995) 283.
[16] A. Faldi, M. Tirrell, T.P. Lodge, Macromolecules 27 (1994) 4176.
[17] A. Faldi, M. Tirrell, T.P. Lodge, E. Von Meerwall, Macromolecules 27 (1994) 4184.
[18] M. Soroush, C. Kravaris, AIChE J. 38 (1992) 1429.
[19] M.F. Ellis, T.W. Taylor, K.F. Jensen, AIChE J. 40 (1994) 445.
[20] T.J. Crowley, K. Choi, J. Process Control 6 (1996) 119.
[21] S.S.S. Chakravarthy, D.N. Saraf, S.K. Gupta, J. Appl. Polym. Sci. 63 (1997) 529.
[22] G.B. Bhargava Ram, D.N. Saraf, S.K. Gupta, J. Appl. Polym. Sci., in press.
[23] R.B. Mankar, D.N. Saraf, S.K. Gupta, J. Polym. Eng., submitted.
[24] T. Peterson, E. Hernandez, Y. Arkun, F.J. Schork, Chem. Eng. Sci. 47 (1992) 737.
[25] G.V. Schulz, G. Harborth, Makromol. Chem. 1 (1947) 106.
[26] S.T. Balke, A.E. Hamielec, J. Appl. Polym. Sci. 17 (1973) 905.
[27] T. Srinivas, S. Sivakumar, S.K. Gupta, D.N. Saraf, Polym. Eng. Sci. 36 (1996) 311.
[28] V. Dua, D.N. Saraf, S.K. Gupta, J. Appl. Polym. Sci. 59 (1996) 749.
[29] T. Srinivas, M. Tech dissertation, Indian Institute of Technology, Kanpur, India, 1994.
[30] D. Braun, H. Cherdron, W. Kern, Techniques of Polymer Synthesis and Characterization, Interscience, New York, 1972.
[31] E.M. McCaffery, Laboratory Preparation for Macromolecular Chemistry, McGraw-Hill, New York, 1970.
[32] J.R. Van Wazar, J.W. Lyons, K.Y. Kim, R.E. Colwell, Viscosity and Flow Measurements, Interscience, New York, 1963.
[33] J. Brandrup, E.H. Immergut (Eds.), Polymer Handbook, 2nd edn., Wiley, New York, 1975.